Publications of the Astronomical Society of the Pacific
108: 944–949, 1996 October

The Flat Sky: Calibration and Background Uniformity in Wide-Field Astronomical Images

FREDERICK R. CHROMEY AND DAVID A. HASSELBACHER

Vassar College Observatory, Poughkeepsie, New York 12601
Electronic mail: chromey@vassar.edu, dahasselbach@vassar.edu

Received 1996 May 16; accepted 1996 July 16

ABSTRACT. Gradients in the surface brightness of the twilight and night sky require careful consideration both in the flat-field calibration and in the subsequent reduction of images that cover a large angular field. We present observations of *BVRI* surface brightness gradients in the twilight sky, and discuss some strategies for the treatment of gradients in the moonlit and dark sky.

1. INTRODUCTION

Charge-coupled devices and other two-dimensional electronic array detectors have widespread application in optical and near-infrared astronomy, but suffer from the fact that not all pixels in the array respond to light with equal efficiency. This defect arises not only because of structural quantum efficiency differences intrinsic to the array itself, but also because of vignetting or other imperfections in the optical system. An observer must therefore make a simple calibration by exposing the complete imaging system to a perfectly uniform luminous field. Pixel-by-pixel variations in the resulting *flat-field* image thus map the detector's efficiency variations, which can therefore be removed from the data frames by an appropriate scaling operation.

In common practice, observers employ one of three different objects as the uniform source for the flat field exposures: (1) the bright twilight sky, (2) the dark night sky, or (3) a nearby object (usually a screen or the inside of the observatory dome) that is uniformly illuminated by a lamp or sky light. Exposures of these sources are usually termed sky, dark, and dome flats, respectively. Each of these has advantages as well as disadvantages, and it is not uncommon to judiciously combine more than one type of flat to optimize the final calibration. This paper notes some limitations of calibrations from twilight and dark flats arising from the nonuniformity of the sky, as well as some considerations regarding real background gradients in properly calibrated data frames.

We were first motivated to undertake this study by our experience with the Burrell Schmidt Telescope (the BST) at Kitt Peak National Observatory. For the past four years we have used this telescope to observe various objects with a wide-field CCD detector (usually the S2KA chip, a 2048 $\times$2048 array with a field of view of 1.1 deg). Since dome flats are highly nonuniform for the BST, we have relied heavily on twilight flats and have found them sufficiently problematic to justify a small observational study of the sky as a broadband calibration source.

In Secs. 2 and 3 below, we present empirical measures of the gradients in the brightness distribution of the twilight sky. We also comment on the size of the gradients to be expected in the dark sky, both in the absence (Sec. 4) and in the presence (Sec. 5) of moonlight. Finally, we discuss the implications of these results for the observer.

2. TWILIGHT OBSERVATIONS

We performed all observations at either the BST or the Vassar College Observatory in Poughkeepsie, New York. It is useful to describe our twilight observations in a spherical coordinate system which uses the local horizon and the solar vertical as reference circles. The solar vertical is the great circle passing through the apparent Sun and the local zenith. The coordinates in this system are the zenith distance z and the azimuth from the solar vertical, A. We use the variable ζ to denote the zenith distance of the Sun itself. Figure 1 illustrates the definitions of these of other angles discussed below. Note that as the Sun executes its diurnal motion, the z,A coordinate system rotates with respect to the usual altitude–azimuth coordinate system.

For the Vassar observations, the camera consisted of a Photometrics thermoelectrically cooled CCD equipped with a 50-mm Nikon lens and the standard observatory *BVRI* filter set (Bessell 1990). The lens was normally stopped down to either $f/4$ or $f/8$. The 512$\times$512 chip has an 11.7 deg field of view in this system. We piggy-back mounted the camera on an 8-in astronomical telescope, which was in turn mounted on an altitude–azimuth mount. Pointing of this system is accurate to about ± 1 deg in each direction.

The apparatus was set up on a roof of the observatory building. For flat-field calibration, we used a white screen illuminated by the bright twilight sky. These flats exhibit no linear gradients, although there is an overall radial gradient of about 5% from center to edge due to camera optics. Observations were conducted on ten clear evenings in the spring and summer of 1994. Changing filters on our instrument was awkward, and we therefore observed only a single color on each evening. Usually, we varied the direction that the camera pointed, but on two occasions simply monitored the sky behavior at a particular (z,A) location from sunset until the end of twilight.

The BST observations were taken at Kitt Peak during 1994 December, 1995 April, and 1995 October. They consisted of a few exposures of the morning and evening twi-

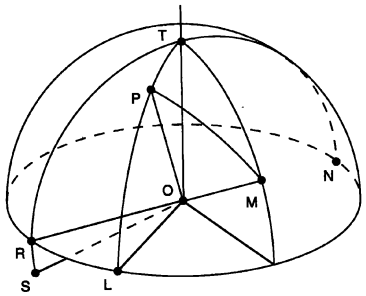

FIG. 1—Definitions of angles. The observer at point O has a local zenith at T, and a horizon circle passing through RLN. The Sun is located at S, on the solar vertical, $SRTN$. Another source, the Moon or bright star, is at M. If point P is observed, then the angles discussed in the text are $z=\angle TOP$, zenith distance of P; $A=\angle ROL$, azimuth from the solar vertical of P; $x=\angle LOP$, elevation of P from the solar horizon, taken to be zero at the sunward horizon and 180° at the opposite horizon; $\zeta=\angle TOS$, zenith distance of the Sun; $z_m=\angle TOM$, zenith distance of the Moon; and $r=\angle POM$, distance between P and the Moon.

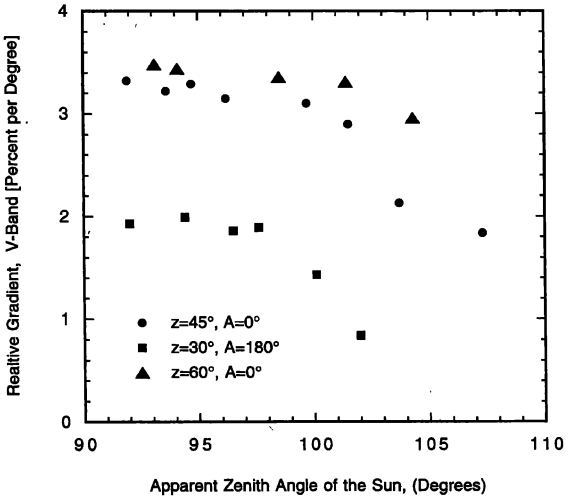

FIG. 2—The values of the absolute magnitude of the relative gradient, g, as a function of solar zenith angle ζ for three different positions on the sky on three different nights. All data on this plot was taken with the Vassar camera in the V band. Note the relative constancy of g with deepening twilight until $\zeta>100°$. Scatter in this figure is due mainly to actual temporal variation in g rather than inaccuracies in camera pointing.

light sky in various directions. Flat fields for these exposures were dark sky flats constructed from program observations during the same runs.

All observations were reduced in the usual way using IRAF and employing either the screen (Vassar) or the dark sky (BST) exposures to generate the flat-field correction. Sky behavior on each twilight frame was characterized by measuring S, sky brightness at the center of the frame, as well as the magnitude and direction of **g**, the relative gradient in the sky brightness at the center,

$$\mathbf{g}=\frac{\nabla S}{S},$$

expressed in percent per degree of arc. We computed the magnitude and direction of **g** by examining iso-intensity contour plots of the individual sky frames. We choose the direction of **g** to be perpendicular to the contour nearest the center, and measured the change in S along a line in that direction. This line was 11 deg long for the Vassar data and 1 deg long for the BST data.

3. TWILIGHT RESULTS

There is a rich literature on "twilight science," much of it directed at probing the structure of the upper atmosphere with twilight observations. Rozenberg (1966) provides a good introduction to and summary of the early work in this area.

Should we expect the gradient in sky brightness at a particular (z,A) location to change with time? It is well known (cf. Rozenberg 1966, pp. 20–27; Tyson and Gal 1993) that the surface brightness of the twilight sky far from the horizon varies exponentially with ζ over the range $93°<\zeta<100°$. We point out that if it is true that in this range of ζ,

$$S(\zeta,z,A)=S_0(z,A)\exp\{-\zeta h(z,A)\},$$

then **g**, the relative brightness gradient, should be independent of ζ (and therefore independent of time) if the time scale for the exponential decay or growth, which is given by the function $h(z,A)$, is independent of position. In fact, the function h does vary with position, but the variation is small except near the horizon. Our measurements indicate that for a given location on the sky, **g** is relatively independent of time. In Fig. 2 we plot the magnitude of **g** as a function of ζ for several locations on the sky (the direction of the vector **g**, generally toward the nearest horizon, is invariant at these locations). Note both the small changes in **g** while $\zeta<100°$, as well as the expected decay from twilight to nighttime values at larger ζ.

Figure 3 shows the behavior of $g(z)$, the magnitude of **g** along the solar vertical. Individual data points in Fig. 3 were taken at various values of ζ (but all less than 100°). The scatter is indicative of the variation of g both during a single twilight, as well as from night to night and observatory to observatory. Note that g drops from large positive values (our convention for a gradient directed toward the Sun) in the bright half-hemisphere to relatively small negative values (gradient toward the antisolar horizon) in the darker half-hemisphere. The behavior of g near both horizons ($z>70°$) is erratic, and we have avoided observations in these regions. Especially relevant to the discussion here is the fact that there is a point near the zenith at which the gradient reaches zero. The location of this null spot appears to vary from night to night, and may also shift position during a single twilight. Location of the null spot may also be a function of wavelength, but our data are not sufficient to test this hypothesis.

4. DARK SKY RESULTS

We have computed $\mathbf{g}(z)$ for a representative dark night sky to compare its uniformity with that of the twilight sky. Figure 4 shows our numerical differentiation of the dark sky model for Mount Graham given by Garstang (1989), as well as values for **g** implied by the observations of Walker (1987)

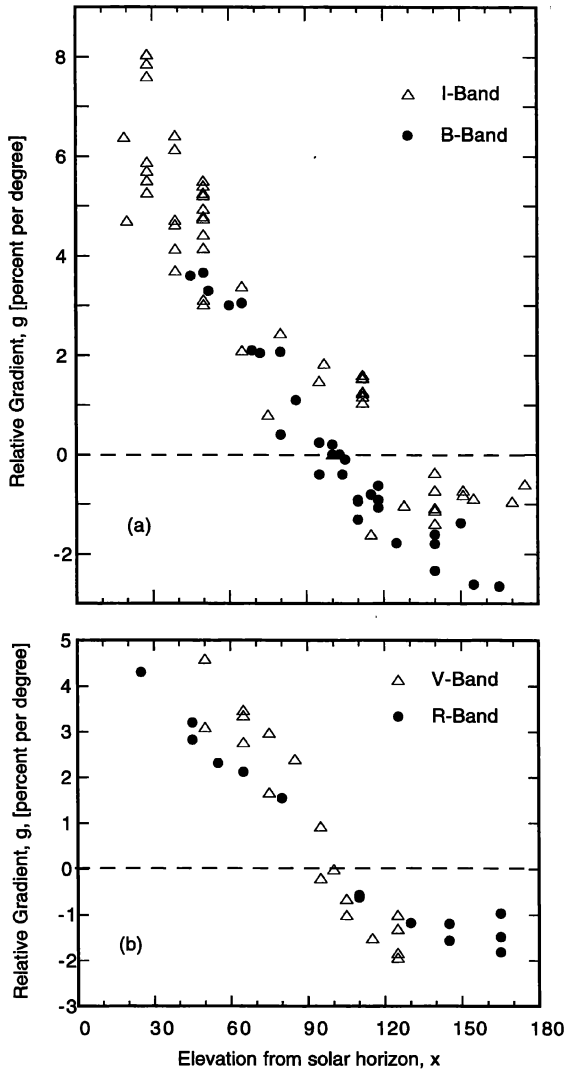

FIG. 3—Values of the magnitude of the relative surface brightness gradient, g, as a function of position on the solar circle. The abscissa, x, is the angle between the horizon point nearest the Sun and the camera pointing, so that the zenith is at 90° and the antisolar horizon is at 180°. Positive values of g correspond to the sky brightening in the solar direction. Measurements (a) in B and I are from both Kitt Peak and Vassar. No systematic differences between the two observatories was apparent in the data. Measurements (b) in V and R are from Vassar only.

at Junipero Serra Peak. In the figure, gradients increase from a value of zero at the zenith to a maximum of a few percent per degree at zenith distances in the 50–80 deg range. All gradients are directed along lines of constant azimuth, with positive gradients implying a sky brightening toward the horizon. We caution that Fig. 4 should be regarded as a lower limit to the $\mathbf{g}(z,A)$ actually encountered at a dark site, since nonuniformities in the background, such as unresolved starlight and zodiacal light, have been averaged. Nor does Fig. 4 consider the effects of light pollution, which will increase the magnitude and possibly change the direction of $\mathbf{g}$. For example, Fig. 5 shows values of sky brightness (not g) measured on the background of I-band data frames taken at high

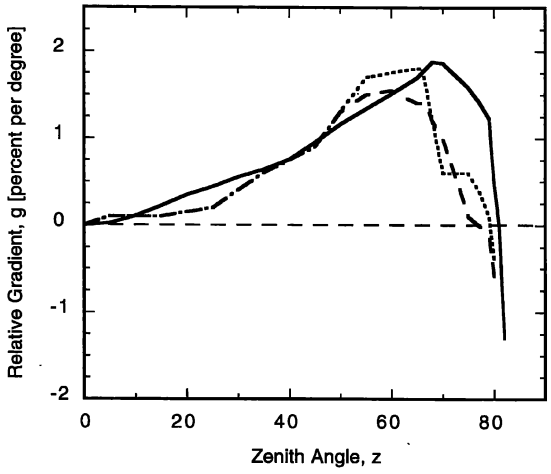

FIG. 4—Values of the relative gradient, g, as a function of zenith distance for the dark sky. Curves were computed by numerical differentiation of the published model of Garstang (1989) for Mount Graham (solid line), and of the V (dotted line) and B (dashed line) observations of the sky at Junipero Serra Peak by Walker (1987).

galactic latitude during two photometric nights at the BST in 1995 October. Although they are by no means definitive, the data do suggest the possibility of gradients over 1% per degree in the direction of Tucson even at modest zenith distances. Gradients of this size are certainly present on many of our data frames. This is in contrast to results reported earlier by Pilachowski et al. (1987).

5. MOONLIGHT RESULTS

We have used the model of Krisciunas and Schaefer (1991) to compute the gradients in sky brightness produced by moonlight alone, and show our results in Fig. 6. The gradients derived from the model depend not only on r, the angular separation between the Moon and the point observed, but also on the zenith distances of the Moon, z_m, and the point on the sky being observed, z. For moonlight alone, the relative gradient $\mathbf{g}$ will be independent of the phase of the moon—in fact, the model applies to any "pointlike" source above the horizon, like the Sun or a bright star. In Fig. 6 we show g as a function of r for two cases: (a) the Moon at the zenith, $z_m=0$, and (b) the Moon low in the sky, $z_m=70$. In case (b), we have only plotted data in the Moon-to-zenith direction, so that the zenith is located at $r=70°$. In the figure, the precipitous increase in g near the Moon (i.e., below $r=9°$) is due to the forward scattering of the moonlight by aerosol particles. We emphasize that Fig. 6 is relevant when the sky brightness is dominated by moonlight, and a more accurate model would sum the contributions of moonlight and the dark sky for a particular site.

6. DISCUSSION

Results in previous sections are representative only. Actual gradients experienced will depend on observatory altitudes and local concentrations of aerosols. In the case of twilight flats, clouds and other conditions hidden by the sun-

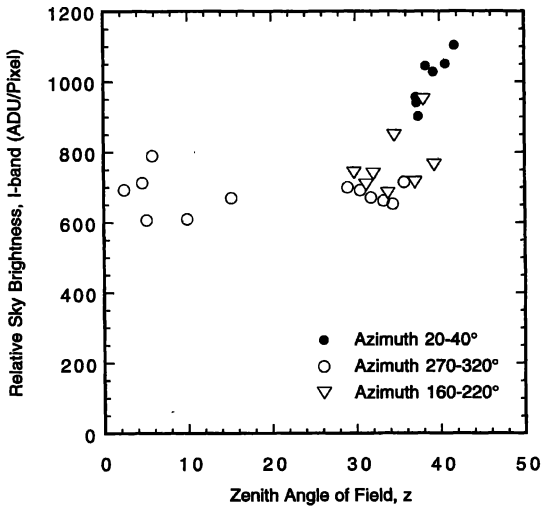

FIG. 5—Surface brightness of the sky background on several 1000-s exposures with the BST at Kitt Peak during two moonless photometric nights. Data have not been corrected for purely temporal effects nor the possible effects of the zodiacal light or unresolved stellar background. Nevertheless, they probably show sky brightening toward Tucson (azimuth about 60°). There were no systematic brightness differences between the two nights, although overall sky brightness changed by small amounts on a time scale of hours.

ward horizon will also have an effect. In the case of the dark sky, the zodiacal light, unresolved stars, and artificial light pollution will cause departures from the plotted values. We make two comments in this section, the first about sky background in data frames, and the second about the proper strategy for flat-field calibration.

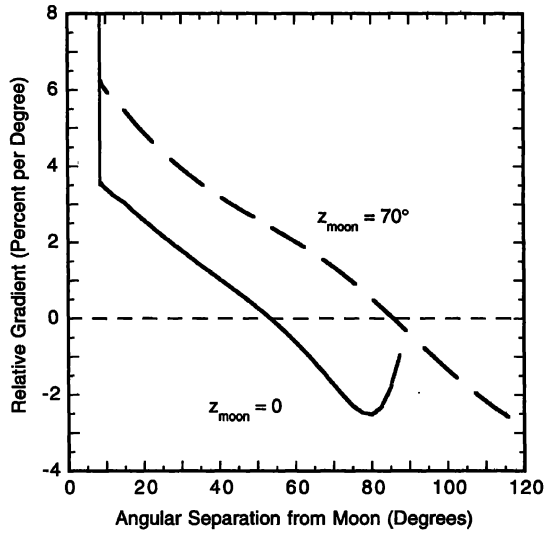

FIG. 6—Values of the relative gradient, g, of the sky illuminated only by a single point source above the horizon. The curves are applicable to the brightly moonlit sky, and show g as a function of r, the separation between the Moon and the point observed. All points are on the lunar vertical. The solid curve is for the Moon at the zenith, and the dashed curve is for the moon near the horizon, at a zenith distance of 70 deg. Computations are based on the models of Krisciunas and Schaefer (1991).

6.1 Sky Background

Consideration of Figs. 4–6 suggests that properly reduced wide-field data frames should display a linear gradient in the intensity of the sky background. The magnitude and direction of the gradient may change from frame to frame as the object changes zenith distance and azimuth. The proper way to deal with this gradient, if it is detectable at all, is to *subtract* a fit to the background from each data frame. For digital aperture photometry, where backgrounds are measured locally (e.g., DAOPHOT), this fitting may be unnecessary, but for surface photometry of extended objects, or for detection of faint objects, it could be very important.

On the other hand, if a gradient creeps into a data frame because of a bad flat field, then the proper correction involves *dividing* by a fit to the background. For any quantitative studies, the difference between subtraction and division could be significant, so it behooves the careful observer either to avoid gradients in the flat-field source, or at least to remove their effects.

6.2 Treating Gradients in the Calibration

The unease produced by a flat-field calibration that is based upon an unflat sky will depend on the width of the field observed and the kind of questions asked about it. Detectors with wide fields of view and projects that demand good photometric accuracy across the field should cause an observer considerable anxiety over sky gradients. Observers in such a state can consider at least three strategies.

(1) Do not use the sky at all, but some kind of dome flat. Although it is difficult to insure uniform illumination of a projector screen, it is sometimes possible to do rather well. At the 15-in telescope at Vassar Observatory, we use a screen illuminated by indirect daylight and obtain gradients of less than 0.5% per degree. Linear gradients and nonaxisymmetric blotches in the screen can be detected by rotation of the detector on the telescope.

(2) Observe the sky, but only where gradients are minimized. The null point for twilight flats is on the solar circle near the zenith, offset toward the antisolar horizon by 0 to 40 deg. The penalty for misjudging the null point is around 1% per degree gradient for every 15 deg off the null. The gradient can increase more rapidly than this near the sunward horizon. That extra flat squeezed out of the brightest parts of the dying twilight will probably have a very large gradient. Sunlight from the null point is highly polarized, although polarization fades with deepening twilight. We have tested the Vassar CCD on an optic bench and find no evidence that the flat-field characteristics of the chip itself are sensitive to different linear polarizations. Our limits are 0.5% pixel to pixel, and 3% across the chip.

The null point for a brightly moonlit sky is on the lunar vertical, 55–90 deg away from the Moon, with the exact angle depending on the Moon's zenith distance and atmospheric conditions. In the case of a "gray" sky (moonlight and sky emission about equal) the Moon will tend to be low in the sky, and the null point will again be near the zenith, but offset in the antilunar direction. Expect huge gradients closer to the Moon than 10 deg.

For a very dark sky free of moonlight and serious artificial light pollution, the null point is at the zenith, and one can expect comparatively small gradients anywhere within 40 deg of this location. A common tactic in the use of the dark sky for calibration is to combine many unregistered data frames (using a median- or high-values rejection algorithm to remove stars and other sources) to compute the flat-field correction. Such dark sky flats reasonably can be expected to have rather low (but probably seldom zero) gradients. The tactic of extracting the flat from the data frames is less successful when an extended object occupies much of the field, and one must then resort to exposures of "blank" sky for the flat field.

In some cases (e.g., narrow bandpasses, short exposures, slow focal ratios) dark sky flats of any kind may exhibit poor photon statistics. Furthermore, the effects of star images, particularly the halos of bright stars, can be difficult to remove completely.

(3) A third strategy is to realize that gradients in dark or twilight sky exposures will be present to some extent, and plan to remove the gradient by first fitting the background of each individual flat with a plane, then dividing the flat by the fit. This assumes that there is no linear gradient in the intrinsic response of the system, or that any such intrinsic characteristic is both well known and stable. Only after removing gradients should the individual flats be combined.

In most cases, it will be necessary to remove the effects of large-scale efficiency variations (due to vignetting, for example) from the individual flats before the gradient due to the sky can be discerned and fit. In this case, a smoothed preliminary flat can be applied as an initial illumination correction to all flats and data.

This strategy of removing gradients from individual flats before combination is essential if one wishes to achieve excellent photometric uniformity as well as to avoid noise from stellar halos. Consider, for example, what might happen in the following scheme, one of our early stumbles on the path to good flats: We reason that if we have pointed the telescope at the same z,A location in evening and morning twilight, even if we miss the null point, we should get similar gradients, but oppositely directed. Combining the morning and evening flats should give us a final result with no gradient. This works, after a fashion, but the combined flat is filled with the faint remains of stellar halos. Figure 7 shows how this arises from the mismatch in backgrounds. The halos would be avoided by gradient removal before image combination. For example, Morrison et al. (1994) have achieved extremely accurate calibrations by a careful reduction that involves fitting the gradients on many of dark sky flats before combination, a rejection algorithm aimed at removing stellar halos, and detailed error modeling.

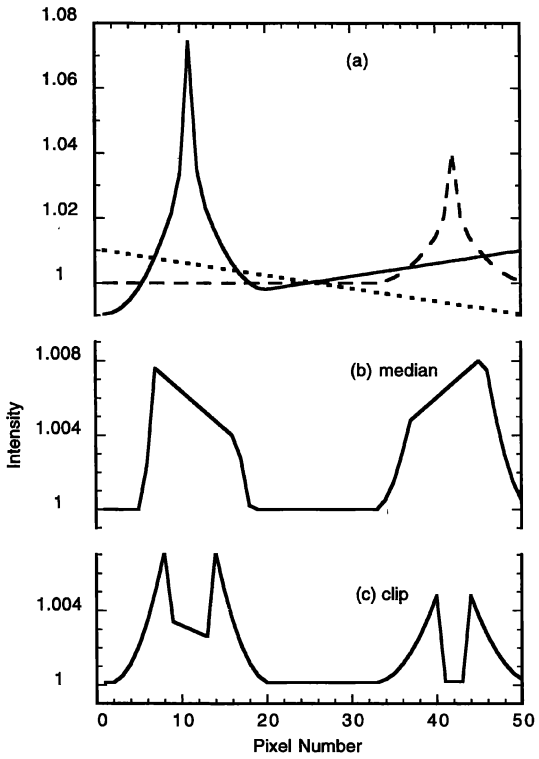

FIG. 7—A schematic representation of the combination of three twilight flats with different background gradients. Intensity traces across the three frames are superimposed in (a). One frame (dashed curve) has no background gradient and contains a star image; another (solid curve) has a 2% overall gradient in the $+x$ direction and also contains a star. The third frame (dotted curve) has a 2% gradient in the $-x$ direction. The median of the three frames is shown in (b). Note the change in scale from (a). Although the gradient has been removed by the median computation, the combined-frame shows faint "pedestals" at the location of the stars. In (c) the three frames have been averaged using a clipping algorithm wherein statisticially suspicious values are ignored, such as *avsigclip* or *ccdclip* in IRAF. In this case, the cores of the stars are nearly removed, but faint wings remain, which will appear as rings in the 2D image.

7. CONCLUSION

Many modern astronomical imagers have fields of view on the order of one degree of arc. Flat-field calibration of these instruments requires the careful observer to consider the likely nonuniformities in traditional calibration sources. Dark, moonlit, and twilight skies all should exhibit a "flat" point where there are no gradients, but it may be difficult to determine the location of this null point with great accuracy. Gradients approaching 1% per degree are not unusual. The proper way to cope with such gradients, if they can be recognized, is to remove them, by division, from individual flat-field exposures before combination. True background gradients may well be present in properly flattened data frames, and can be removed by subtraction.

The authors wish to thank Heather Morrison and Frank Winkler for useful discussions, and the anonymous referee for very helpful suggestions. Leslie Sherman, Dan Pierkowski, and Jeff Kern assisted with some of the Vassar observations. The Burrell Schmidt Telescope is owned by Case Western Reserve University and operated by the Kitt Peak National Observatory. We are pleased to acknowledge the support of the W. H. Keck Foundation, through a grant to the Keck Northeast Astronomy Consortium, as well as the support of the Vassar College General Research Fund.

REFERENCES

Bessell, M. S. 1990, PASP, 102, 1181
Garstang, R. H. 1989, PASP, 101, 306
Krisciunas, K., and Schaefer, B. E. 1991, PASP, 103, 1033
Morrisson, H. L., Boroson, T. A., and Harding, P. 1994, AJ, 108, 1191
Pilachowski, C. A., Africano, J. L., Massey, P., Goodrich, B. D., and Binkert, W. S. 1987, PASP, 99, 1149
Rozenberg, G. V. 1966, Twilight, A Study in Atmospheric Optics, translated from the Russian by R. B. Rodman (New York, Plenum)
Tyson, N. D., and Gal, R. R. 1993, AJ, 105, 1206
Walker, M. F. 1987, in Identification, Optimization and Protection of Optical Telescope Sites, ed. R. L. Millis, O. G. Franz, H. D. Ables, and C. C. Dahn (Flagstaff, Lowell Observatory), p. 128